

VALIDATION OF DISCRETE FRAMEWORK FOR FIBER REINFORCEMENT

Chunling Li, University of Texas at Austin, USA
Jorge G. Zornberg, University of Texas at Austin, USA

Li, C., and Zornberg, J.G. (2003). "Validation of Discrete Framework for Fiber Reinforcement." Proceedings of the 2003 North American Conference on Geosynthetics, Winnipeg, Canada, September 28 - October 1 (CD-ROM).

ABSTRACT: An experimental study was conducted to validate a previously-proposed discrete methodology for the design of fiber-reinforced soil. The analysis of shear strength of fiber-reinforced soil using a discrete approach can be conducted by independent characterization of soil specimens and of fiber specimens since the contributions of soil and fibers are treated separately, and the non-conventional laboratory testing of the composite fiber-reinforced soil specimens in the traditional composite approach can be avoided. A fiber-induced distributed tension can be defined for use in stability analyses using the proposed discrete framework.

The experimental testing program involves tensile testing of fibers as well as triaxial testing of unreinforced and fiber-reinforced specimens. The triaxial tests were conducted using both sand and clay soils, reinforced with different types of polypropylene fibers. As predicted by the discrete framework, the fiber-induced distributed tension was observed to be proportional to the fiber content and fiber aspect ratio when failure is characterized by pullout of individual fibers. Overall, very good agreement was found between experimental and predicted results for both sand and clay soils. Specifically, the discrete framework was able to accurately predict the contribution of randomly distributed fibers for the various soil types, aspect ratios, and fiber contents considered in the experimental testing program.

RÉSUMÉ: Une étude expérimentale a été dirigée pour valider une méthodologie discrète précédemment proposée pour la conception de sol fibre renforcé. L'analyse de force de cisailles d'utilisation de sol fibre renforcé une approche discrète peut être dirigée par la caractérisation indépendante de spécimens de sol et de spécimens de fibre puisque les contributions de sol et les fibres est séparément traitée, et le laboratoire non conventionnel essayant des spécimens de sol fibre renforcés composés dans l'approche composée traditionnelle peut être évité. Une tension distribuée fibre persuadé peut être définie pour l'usage dans la stabilité analyse l'utilisation de la structure discrète proposée.

Le programme essayant expérimental implique l'essai extensible de fibres de même que l'essai triaxial de spécimens de unreinforced et fibre renforcé. Les tests triaxiaux ont été dirigés le sable d'utilisation et les sols d'argile, renforcés avec les types différents de fibres de polypropylène. Comme prédit par la structure discrète, le fibre persuadé la tension distribuée a été observée pour être proportionnelle au contenu de fibre et à la proportion d'aspect de fibre quand l'échec est caractérisé par individuelles retraite de fibres individuel. Général, le très bon accord a été trouvé entre les résultats expérimentaux et prédits pour les sols de sable et argile. En particulier, la structure discrète pouvait précisément prédire la contribution de fibres au hasard distribuées pour les divers types de divers sol, les diverses proportions d'aspect, et les contenus de fibre considérés dans le programme essayant expérimental.

1. INTRODUCTION

Fiber reinforcement has become a promising solution to the stabilization of thin soil veneers and localized repair of failed slopes. Randomly distributed fibers can maintain strength isotropy and avoid the existence of the potential planes of weakness that can develop parallel to continuous planar reinforcement elements. The design of fiber-reinforced soil slopes has typically been performed using composite approaches, where the fiber-reinforced soil is considered a single homogenized material. Accordingly, fiber-reinforced soil design has required non-conventional laboratory testing of composite fiber-reinforced soil specimens which has discouraged implementation of fiber-reinforcement in engineering practice.

Several composite models have been proposed to explain the behavior of randomly distributed fibers within a soil mass (Maher and Gray, 1990, Michalowski and Zhao, 1996, Ranjan et al., 1996). The mechanistic models proposed by Gray and Ohashi (1983) and Maher

and Gray (1990) quantify the "equivalent shear strength" of the fiber-reinforced composite as a function of the thickness of the shear band that develops during failure. Information needed to characterize shear band development for these models is, however, difficult to quantify (Shewbridge and Sitar, 1990). Common findings from the various testing programs implemented to investigate composite models include: (i) randomly distributed fibers provide strength isotropy in a soil composite; (ii) fiber inclusions increase the "equivalent" shear strength within a reinforced soil mass; and (iii) the "equivalent" strength typically shows a bilinear behavior, which was experimentally observed by testing of comparatively weak fibers under a wide range of confining stresses.

A discrete approach for the design of fiber-reinforced soil slopes was recently proposed to characterize the contribution of randomly distributed fibers to stability (Zornberg, 2002). In this approach, fiber-reinforced soil is characterized as a two-component (soil and fibers) material. Fibers are treated as discrete elements that

contribute to stability by mobilizing tensile stresses along the shear plane. Consequently, independent testing of soil specimens and of fiber specimens, but not of fiber-reinforced soil specimens, can be used to characterize fiber-reinforced soil performance.

This paper initially reviews the main concepts of the discrete approach and subsequently validates the framework for design purposes.

2. DISCRETE FRAME WORK FOR FIBER REINFORCEMENT

2.1 Background

The volumetric fiber content, χ , used in the proposed discrete framework is defined as:

$$\chi = \frac{V_f}{V} \quad [1]$$

where V_f is the volume of fibers and V is the control volume of fiber-reinforced soil.

The gravimetric fiber content, χ_w , typically used in construction specifications, is defined as:

$$\chi_w = \frac{W_f}{W_s} \quad [2]$$

where W_f is the weight of fibers and W_s is the dry weight of soil.

The dry unit weight of the fiber-reinforced soil composite, γ_d , is defined as:

$$\gamma_d = \frac{W_f + W_s}{V} \quad [3]$$

The contribution of fibers to stability leads to an increased shear strength of the "homogenized" composite reinforced mass. However, the reinforcing fibers actually work in tension and not in shear. A major objective of the discrete framework is to explicitly quantify the fiber-induced distributed tension, t , which is the tensile force per unit area induced in a soil mass by randomly distributed fibers.

Specifically, the magnitude of the fiber-induced distributed tension is defined as a function of properties of the individual fibers. In this way, as in analysis involving planar reinforcements, limit equilibrium analysis of fiber-reinforced soil can explicitly account for tensile forces.

The interface shear strength of individual fibers can be expressed as:

$$f_f = c_{i,c} \cdot c + c_{i,\phi} \cdot \tan \phi \cdot \sigma_{n,ave} \quad [4]$$

where c and ϕ are the cohesive and frictional components of the soil shear strength and $\sigma_{n,ave}$ is the average normal stress acting on the fibers. The interaction coefficients, $c_{i,c}$ and $c_{i,\phi}$, commonly used in soil reinforcement literature for continuous planar reinforcement, is adopted herein to relate the interface shear strength to the shear strength of the soil. The interaction coefficients are defined as:

$$c_{i,c} = \frac{a}{c} \quad [5]$$

$$c_{i,\phi} = \frac{\tan \delta}{\tan \phi} \quad [6]$$

where a is the adhesive component of the interface shear strength between soil and the polymeric fiber, $\tan \delta$ is the skin-frictional component.

The pullout resistance of a fiber of length l_f should be estimated over the shortest side of the two portions of a fiber intercepted by the failure plane. The length of the shortest portion of a fiber intercepted by the failure plane varies from zero to $l_f/2$. Statistically, the average embedment length of randomly distributed fibers, $l_{e,ave}$, can be analytically defined by:

$$l_{e,ave} = \frac{l_f}{4} \quad [7]$$

where l_f is total length of the fibers.

The average pullout resistance can be quantified along the average embedment length, $l_{e,ave}$, of all individual fibers crossing a soil control surface A . The ratio between the total cross sectional area of the fibers A_f and the control surface A is assumed to be defined by the volumetric fiber content χ . That is:

$$\chi = \frac{A_f}{A} \quad (8)$$

When failure is governed by the pullout of the fibers, the fiber-induced distributed tension, t_p , is defined as the average of the tensile forces inside the fibers over the control area A . Consequently, t_p can be estimated as:

$$t_p = \chi \cdot \eta \cdot (c_{i,c} \cdot c + c_{i,\phi} \cdot \tan \phi \cdot \sigma_{n,ave}) \quad [9]$$

where η is the aspect ratio defined as:

$$\eta = \frac{l_f}{d_f} \quad [10]$$

where d_f is the equivalent diameter of the fiber.

When failure is governed by the yielding of the fibers, the distributed tension, t_i , is determined from the tensile strength of the fiber:

$$t_i = \chi \cdot \sigma_{f,ult} \quad [11]$$

where $\sigma_{f,ult}$ is the ultimate tensile strength of the individual fibers.

The fiber-induced distributed tension t to be used in the discrete approach to account for the tensile contribution of the fibers in limit equilibrium analysis is:

$$t = \min(t_p, t_i) \quad [12]$$

The critical normal stress, $\sigma_{n,crit}$, which defines the change in the governing failure mode, is the normal stress at which failure occurs simultaneously by pullout and tensile breakage of the fibers. That is, the following condition holds at the critical normal stress:

$$t_i = t_p \quad [13]$$

An analytical expression for the critical normal stress can be obtained as follows:

$$\sigma_{n,crit} = \frac{\sigma_{f,ult} - \eta \cdot c_{i,c} \cdot c}{\eta \cdot c_{i,\phi} \cdot \tan \phi} \quad [14]$$

2.2 Equivalent Shear Strength of Fiber-Reinforced Soil

As in analyses involving planar inclusions, the orientation of the fiber-induced distributed tension should also be identified or assumed. Specifically, the fiber-induced distributed tension can be assumed to act: a) along the failure surface so that the discrete fiber-induced tensile contribution can be directly "added" to the shear strength contribution of the soil in a limit equilibrium analysis; b) horizontally, which would be consistent with design assumptions for reinforced soil structures using planar reinforcements; and c) in a direction somewhere between the initial fiber orientation (which is random) and the orientation of the failure plane.

This equivalent shear strength of fiber-reinforced specimens can be defined as a function of the fiber-induced distributed tension t , and the shear strength of the unreinforced soil, S :

$$S_{eq} = S + \alpha \cdot t = c + \sigma_n \tan \phi + \alpha \cdot t \quad [15]$$

where α is an empirical coefficient that accounts for the orientation of fiber and the efficiency of the mixing of fibers. α is equal to 1, if the fibers are randomly distributed and working with 100% efficiency, otherwise α should be smaller than 1.

Depending on whether the mode of failure is fiber pullout or yielding, the equivalent shear strength can be derived by combining (9) or (11) with (15). It should be noted that the average normal stress acting on the fibers, $\sigma_{n,ave}$, does not necessarily equal the normal stress on the shear plane σ_n . For randomly distributed fibers, $\sigma_{n,ave}$ could be represented by the octahedral stress component. However, a sensitivity evaluation undertaken using typical ranges of shear strength parameters show that $\sigma_{n,ave}$ can be approximated by σ_n without introducing significant error.

Accordingly, the following expressions can be used to define the equivalent shear strength when failure is governed by fiber pullout:

$$S_{eq,p} = c_{eq,p} + (\tan \phi)_{eq,p} \cdot \sigma_n \quad [16]$$

$$c_{eq,p} = (1 + \alpha \cdot \eta \cdot \chi \cdot c_{i,c}) \cdot c \quad [17]$$

$$(\tan \phi)_{eq,p} = (1 + \alpha \cdot \eta \cdot \chi \cdot c_{i,\phi}) \cdot \tan \phi \quad [18]$$

Equivalently, the following expressions can be obtained to define the equivalent shear strength when failure is governed by tensile breakage of the fibers:

$$S_{eq,t} = c_{eq,t} + (\tan \phi)_{eq,t} \cdot \sigma_n \quad [19]$$

$$c_{eq,t} = c + \alpha \cdot \chi \cdot \sigma_{f,ult} \quad [20]$$

$$(\tan \phi)_{eq,t} = \tan \phi \quad [21]$$

The above expressions yield a bilinear shear strength envelope, which is shown in Figure 1.

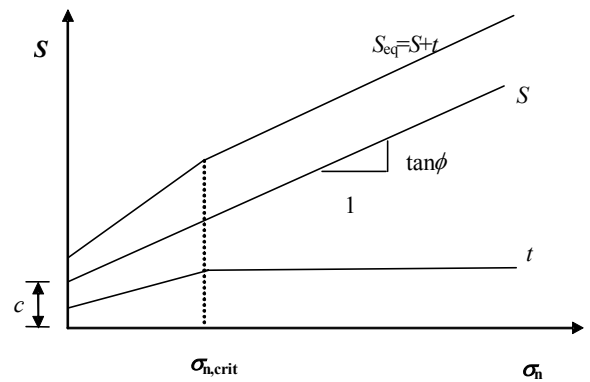


Figure 1 Representation of the equivalent shear strength according to the discrete approach

3. EXPERIMENTAL VALIDATION

3.1 Experimental testing program

A triaxial compression testing program on fiber-reinforced soil was implemented to validate the proposed discrete framework. Both cohesive and granular soils were used in the testing program, and the soil properties were summarized in Table 1.

Table 1 Summary of soil properties

Soil type	Soil 1	Soil 2
USCS classification	SP	CL
LL %	-	49
PL %	-	24
IP %	-	25
% Fines	1.4	82.6

The tests were conducted using commercially available polypropylene fibers, and the properties of fibers were summarized in Table 2. A series of tensile test were performed in general accordance with ASTM D2256-97 to evaluate the ultimate tensile strength of fibers. The average tensile strength of the fibers was approximately 425,000 kPa.

The triaxial testing program involved consolidated drained (CD) tests for SP soils and consolidated undrained (CU) tests for CL soils. The specimens have a diameter of 71 mm and a minimum length-to-diameter ratio of 2. The CU tests were performed in general accordance with ASTM D4767, and the specimens were back pressure saturated and the pore water pressure was measured. The unreinforced tests of SP soil yielded an effective shear strength envelope defined by cohesion of 6.1 kPa and friction angle of 34.3°, while the cohesion and friction angle of CL soil were 12.0 kPa and 31.0° respectively.

Table 2 Summary of fiber properties

	SP tests	CL tests
Linear density (denier)	1000 & 360	2610
Fiber content (%)	0.2 & 0.4	0.2 & 0.4
Length of fibers (mm)	25 & 51	25 & 51
Type of fiber	fibrillated & tape	fibrillated

The governing failure mode for the polymeric fibers used in this investigation is pullout because of the comparatively high tensile strength and short length of the fibers. Accordingly, the triaxial testing program conducted in this study focuses only on the first portion of the bilinear strength envelope shown in Figure 1.

3.2 Stress-strain behavior

SP soils reinforced with fibers

Figure 2 shows the stress-strain behavior of SP soil specimens reinforced with 360 denier fibers, and placed

at gravimetric fiber contents of 0, 0.2 and 0.4 %. Specimens were tested under confining pressure of 70 kPa. The peak deviator stress increases approximately linearly with increasing fiber content, which is consistent with the discrete framework (see equation (9)). The post-peak shear strength loss is smaller in the reinforced specimens than in the unreinforced specimens. However, the initial portions of the stress-strain curves of the reinforced and unreinforced specimens are approximately similar. Accordingly, the soil appears to take most of the applied load at small strain levels, while the load resisted by the fibers is more substantial at higher strain level. The larger strain corresponding to the peak deviator stress displayed by the fiber-reinforced specimens suggests that fibers increase the ductility of the reinforced soil specimen. These findings are confirmed in Figure 3, which shows the test results obtained under higher confining stress (140 kPa).

The effect of fiber length on the stress-strain behavior is shown in Figure 4. The specimens were prepared using fibers with a different fiber type (1000 denier) than that used in the tests shown in Figures 2 and 3. The specimens were prepared using the same gravimetric fiber content, but with varying fiber length. The specimens reinforced with longer (50 mm) fibers displayed higher shear strength. The peak deviator stress increases linearly with increasing aspect ratio, which is also consistent with the trend indicated by equation (9). The strain corresponding to the peak strength increases with increasing fiber length. When the governing failure mode is pullout, the fiber-induced distributed tension reaches its peak when the pullout resistance is fully mobilized. For longer fibers, it usually requires a larger interface shear deformation to fully mobilize the interface strength. Consequently, the macroscopic axial strain at peak stress should be larger for specimen reinforced with longer fibers. Figure 5 shows a similar trend for the case of tests conducted under higher confining pressures.

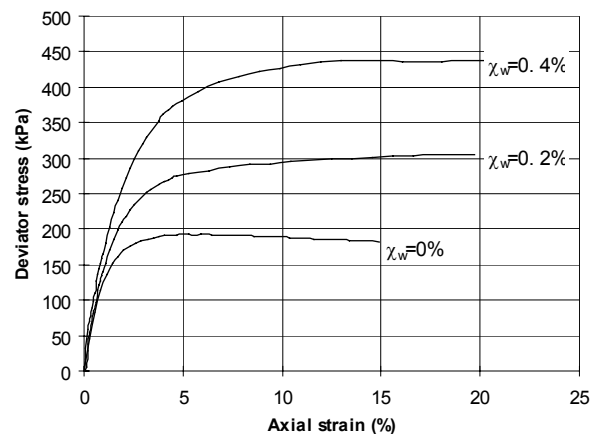


Figure 2 Stress-strain behavior of specimens prepared using $\chi_w=0, 0.2$ and 0.4% with $l_f=25$ mm fibers (360 denier), $\sigma_3=70$ kPa, Soil 1

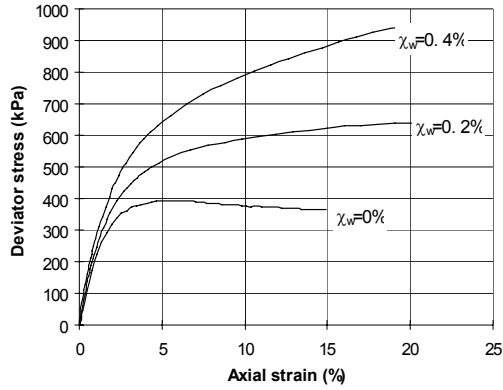


Figure 3 Stress-strain behavior of specimens prepared using $\chi_w=0, 0.2$ and 0.4% with $l_f=25$ mm fibers (360 denier), $\sigma_3=140$ kPa, Soil 1

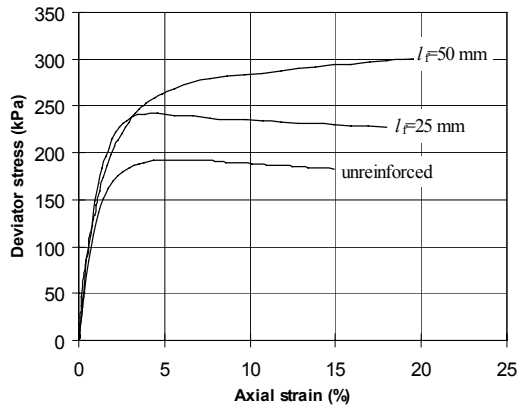


Figure 4 Stress-strain behavior of specimen prepared using $\chi_w=0.2$ %, with $l_f=25$ mm and 50 mm fibers (1000 denier), $\sigma_3=70$ kPa, Soil 1

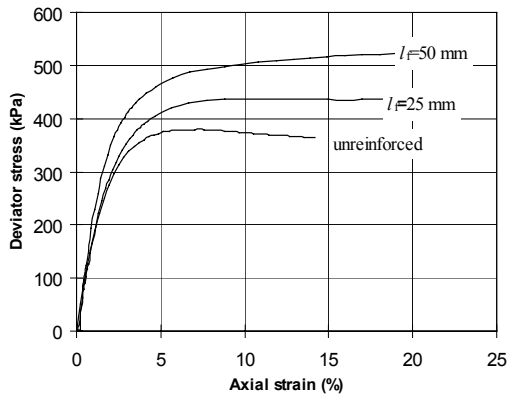


Figure 5 Stress-strain behavior of specimen prepared using $\chi_w=0.2$ %, with $l_f=25$ mm and 50 mm fibers (1000 denier), $\sigma_3=140$ kPa, Soil 1

CL soils reinforced with fibers

Figure 6 compares the stress-strain behavior of both unreinforced and fiber-reinforced specimen using soil 2. The reinforced specimen were prepared at $\chi_w=0.2\%$, using 2-inch long 2610 denier fibers. Both specimens were compacted at optimum moisture content to 90% of the maximum dry density achieved in the standard Proctor test as specified in ASTM D 698, and tested under confining pressure $\sigma_3=98$ kPa. Due to the undrained test condition, the effective confining stress changes with the excess pore water pressure induced in the process of shearing. The peak shear strength was selected in terms of the maximum value of (σ_1'/σ_3') . The increment of deviator stress due to fiber addition is not as obvious as in the case of SP sand. However, the pore water pressure generated during shearing is larger for reinforced specimen than for unreinforced specimen (see Figure 7). Consequently the effective confining stress inside the reinforced specimen is smaller than that inside the unreinforced specimen. The fiber-reinforced specimen achieved equal or higher peak deviator stress than the unreinforced specimen under a lower effective confining stress. This shows that the addition of fibers increases the shear strength of the reinforced specimen. Since positive water pressure is associated with the tendency of volume shrinkage, this observation shows that fiber reinforcement restrains the dilatancy of the reinforced soil. Other researchers (Michalowski and Cermak, 2003, Consoli et al., 1998) reported that fiber-reinforced specimens displayed smaller volume dilatation than unreinforced specimen in consolidated drained (CD) test. This observation confirms their findings in a different test condition.

Similar observation can be made from Figures 8 and 9, which shows the stress-strain behavior and the pore water pressure evolution obtained using 25-mm fibers placed at 0.2% and 0.4% gravimetric fiber contents. As the fiber content increases, the pore water pressure generated during undrained shearing also increases.

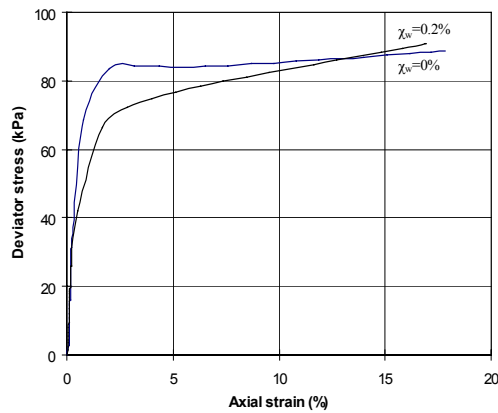


Figure 6 Stress-strain behavior of specimens prepared using $\chi_w=0, 0.2$ %, with $l_f=50$ mm fibers (2610 denier), $\sigma_3=98$ kPa, Soil 2

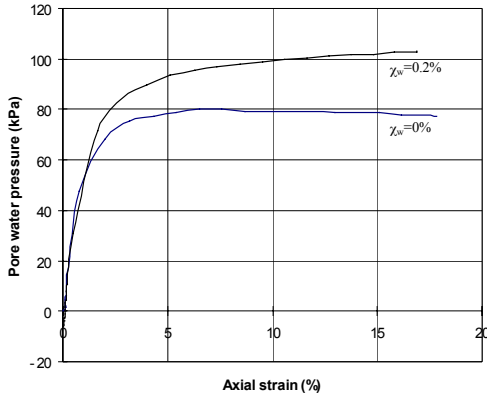


Figure 7 Excess pore water pressure of specimens prepared using $\chi_w=0, 0.2 \%$, with $l_f=50$ mm fibers (2610 denier), $\sigma_3=98$ kPa, Soil 2

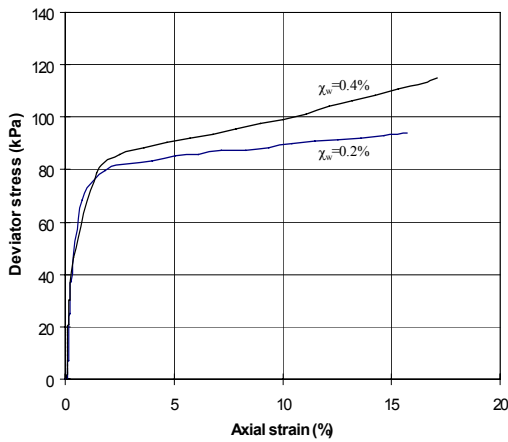


Figure 8 Stress-strain behavior of specimens prepared using $\chi_w=0.2, 0.4 \%$, with $l_f=25$ mm fibers (2610 denier), $\sigma_3=116$ kPa, Soil 2

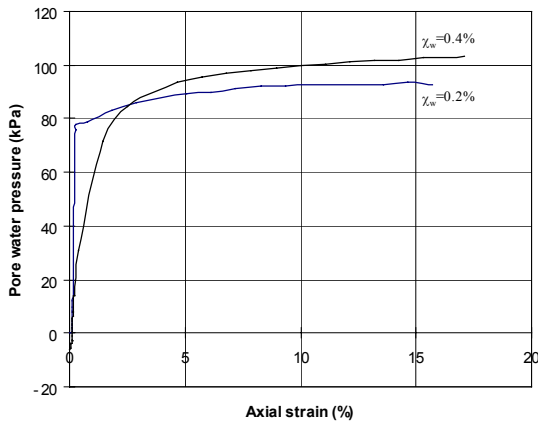


Figure 9 Excess pore water pressure of specimens prepared using $\chi_w=0.2, 0.4 \%$, with $l_f=25$ mm fibers (2610 denier), $\sigma_3=116$ kPa, Soil 2

3.3 Shear strength behavior

Equations (16) through (18) were used to predict the equivalent shear strength for fiber-reinforced specimens. Interaction coefficients ($c_{i,c}$ and $c_{i,\phi}$) of 0.8 are assumed in the analyses conducted in this study. The interface shear strength obtained from pullout test results conducted on woven geotextiles was considered representative of the interface shear strength on individual fibers. For practical purposes, interaction coefficients can be selected from values reported in the literature for continuous planar reinforcements. This is because pullout tests conducted using a variety of soils and planar geosynthetics have been reported to render interaction coefficient values falling within a narrow range (Koutsourais et al., 1998, Michalowski and Cermak, 2003). α is assumed to be 1.0 for randomly distributed fibers. Table 3 summarized the values of parameters used in the analyses.

Table 3 Summary of parameters used in the prediction

	α	ϕ ($^\circ$)	c (kPa)	$c_{i,c}$	$c_{i,\phi}$
Soil 1	1.0	34.3	6.1	0.8	0.8
Soil 2	1.0	31.0	12.0	0.8	0.8

The effect of fiber content on shear strength is shown in Figure 10, which compares the experimental data and predicted shear strength envelopes obtained from Soil 1 using 25 mm fibers with linear density of 360 denier placed at fiber contents of 0.0%, 0.2%, and 0.4%. The experimental results show a clear increase in equivalent shear strength with increasing fiber content. No major influence of fibrillation is perceived in the results of the testing program. The shear strength envelope for the unreinforced specimens was defined by fitting the experimental data. However, the shear strength envelopes shown in the figure for the reinforced specimens were predicted analytically using the proposed discrete framework. A very good agreement is observed between experimental data points and predicted shear strength envelopes. As predicted by the discrete framework, the distributed fiber-induced tension increases linearly with the volumetric fiber content. Similar observation can be made in Figure 11, which shows the results obtained from Soil 2 using 50-mm-long fibers with linear density of 2610 denier.

The effect of fiber aspect ratio on shear strength is shown in Figure 12, which compares the experimental and predicted shear strength envelopes of specimens of Soil 1 placed at $\chi_w=0.2\%$, with 25 and 50 mm-long fibers. As predicted by the discrete framework, increasing the fiber length increases the pullout resistance of individual fibers, and results in a higher fiber-induced distributed tension. Consequently, for the same fiber content, specimens reinforced with longer fibers will have higher equivalent shear strength. This trend agrees well with the experimental data. Similar observation can be made from Figure 13, which shows the results obtained from Soil 2 using 25 mm and 50 mm-long fibers and placed at $\chi_w=0.4\%$.

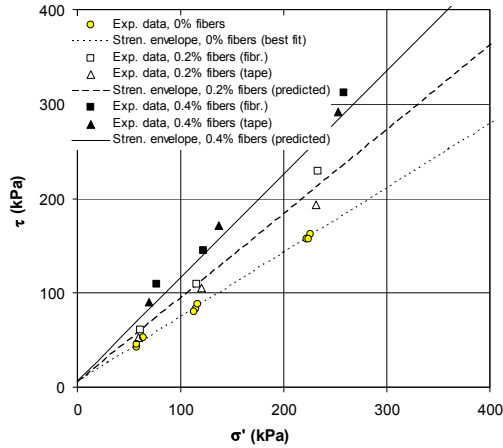


Figure 10 Comparison between predicted and experimental shear strength results for specimens reinforced at $\chi_w=0, 0.2\%, 0.4\%$ with 25 mm-long fibers (360 denier), Soil 1

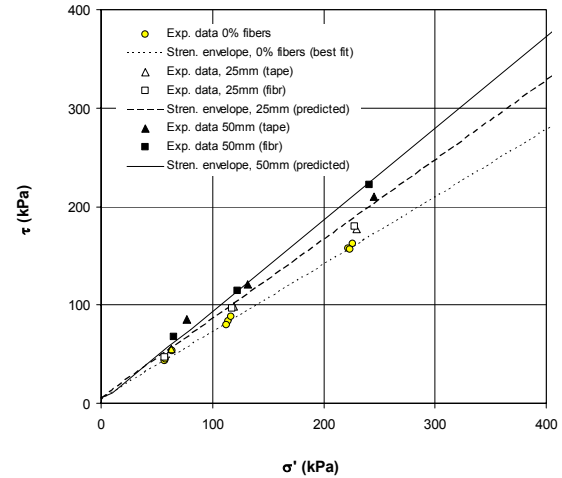


Figure 12 Comparison between predicted and experimental shear strength results for specimens reinforced at $\chi_w=0.2\%$, with 25 mm-long and 50 mm-long fibers (1000 denier), Soil 1

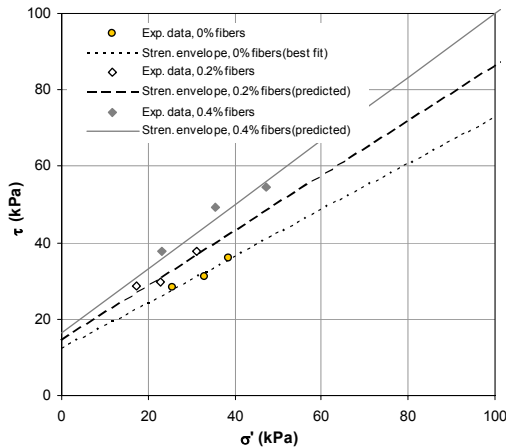


Figure 11 Comparison between predicted and experimental shear strength results for specimens reinforced at $\chi_w=0, 0.2\%, 0.4\%$ with 50 mm-long fibers (2610 denier), Soil 2

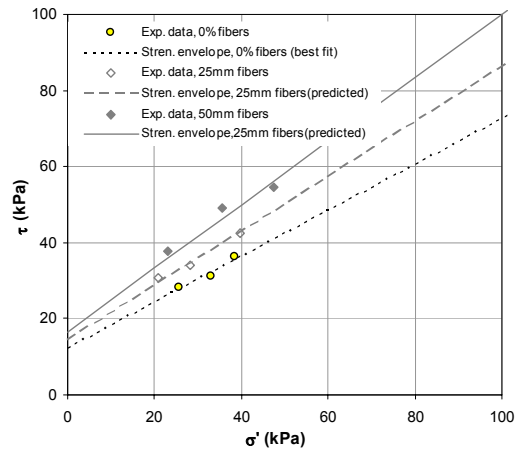


Figure 13 Comparison between predicted and experimental shear strength results for specimens reinforced at $\chi_w=0.4\%$, with 25 mm-long and 50 mm-long fibers (2610 denier), Soil 2

3.4 Combined effect of aspect ratio and fiber content

Additional insight into the validity of the proposed discrete approach can be obtained by comparing the results obtained for specimens reinforced with 50 mm-long fibers placed at a fiber content of 0.2% with those obtained for specimens reinforced with 25 mm-long fibers placed at a fiber content of 0.4%. That is specimens with a constant value of $(\chi_w \cdot \eta)$. As inferred from inspection of equation (9) the fiber-induced distributed tension is directly proportional to both the fiber content and the fiber aspect ratio. Consequently, the predicted equivalent shear strength parameters for the above combinations of fiber length and fiber content are the same. Figures 14 and 15 combine these experimental results.

The good agreement between experimental results and predicted values provides additional evidence of the suitability of the proposed discrete approach. From the practical standpoint, it should be noted that using 50 mm-long fibers placed at a fiber content of 0.2% corresponds to half the reinforcement material than using 25 mm-long fibers placed at a fiber content of 0.4%. That is, for the same target equivalent shear strength the first combination leads to half the material costs than the second one. It is anticipated, though, that difficulty in achieving good fiber mixing may compromise the validity of the relationships developed herein for comparatively high aspect ratios (i.e. comparatively long fibers) and for comparatively high fiber contents. The fiber content or fiber length at which the validity of these relationships is compromised should be further evaluated. Nonetheless, good mixing was achieved for the fiber contents and fiber lengths considered in this investigation, which were

selected based on values typically used in geotechnical projects.

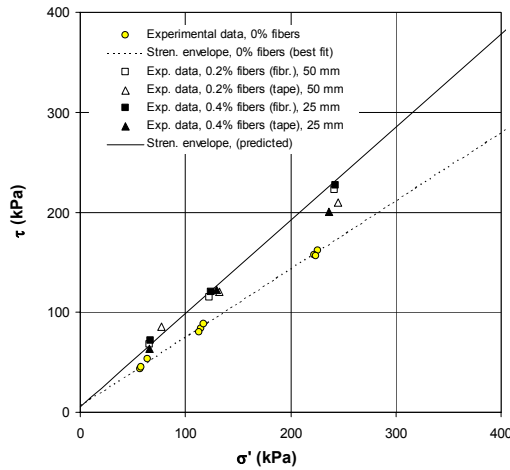


Figure 14 Consolidated shear strength results for specimen reinforced with 50 mm-long fibers (1000 denier) placed at $\chi_w = 0.2\%$ and 25 mm fibers placed at $\chi_w = 0.4\%$, Soil 1

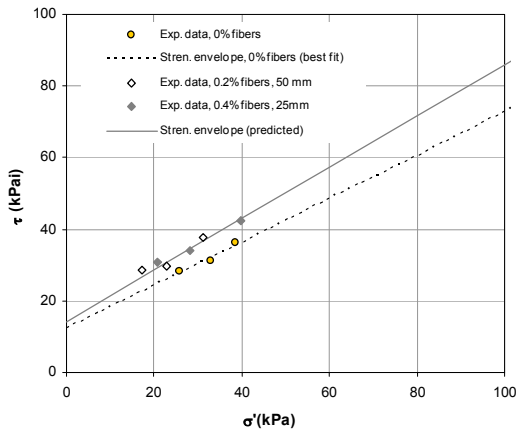


Figure 15 Consolidated shear strength results for specimen reinforced with 50 mm-long fibers (2610 denier) placed at $\chi_w = 0.2\%$ and 25 mm fibers placed at $\chi_w = 0.4\%$, Soil 2

Figure 16 shows the stress-strain behavior of specimen reinforced with 50 mm fibers placed at $\chi_w = 0.2\%$ and 25 mm fibers placed at $\chi_w = 0.4\%$. While the discrete approach was developed only to predict the shear strength response, the results in the figure show that fiber-reinforced specimens prepared using a constant value of $(\chi_w \cdot \eta)$ display similar stress-strain behavior. This similar response is observed for both fibrillated and tape fibers, suggesting that the fibrillation procedure does not have a significant impact on the mechanical response of fiber-reinforced soil. The experimental results suggest that the proportionality of shear strength with the fiber content and fiber aspect ratio predicted by the discrete framework can be extrapolated to the entire stress-strain response of fiber-reinforced specimens.

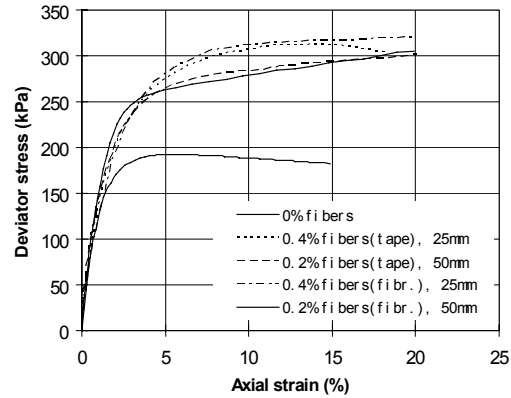


Figure 16 Comparison between stress-strain behavior for specimen reinforced with 50mm fibers (1000 denier) placed at $\chi_w = 0.2\%$ and 25 mm fibers placed at $\chi_w = 0.4\%$, $\sigma_3 = 70$ kPa

4. CONCLUSIONS

The discrete approach for fiber-reinforced soil was validated in this investigation using experimental data from a triaxial testing of both sand and clay. The effect of fiber reinforcement on stress-strain behavior and shear strength was investigated and compared with the analytical results of the discrete approach. The main conclusions drawn from this investigation are:

- The addition of fibers can significantly increase the peak shear strength and limit the post peak strength loss of both cohesive and granular soil. An increase in fiber content leads to increasing strain at failure and, consequently, to a more ductile behavior.
- The fiber reinforcement tends to restrain the volume dilation of the soil in drained condition, or equivalently, increase the positive water pressure in undrained condition.
- The peak shear strength increases with increasing aspect ratio. The strain at peak deviator stress increases with increasing fiber aspect ratio.
- As predicted by the discrete framework, the experimental results confirmed that the fiber-induced distributed tension increases linearly with fiber content and fiber aspect ratio when failure is characterized by pullout of individual fibers.
- Experimental results conducted using specimens with a constant $(\chi_w \cdot \eta)$ value show not only the same shear strength but also display a similar stress-strain behavior.
- If good mixing can be achieved, fibers with comparatively high aspect ratio can lead to lower fiber contents while reaching the same target equivalent shear strength, resulting in savings of reinforcement material.
- Overall, for both sand and clay specimens, the discrete approach was shown to predict accurately the shear strength obtained experimentally using specimens reinforced with polymeric fibers tested under confining stresses typical of slope stabilization projects.

REFERENCES

- Consoli N.C., Prietto P.D.M., Ulbrich L.A. 1998, "Influence of Fiber and Cement Addition on Behavior of Sandy Soil", *ASCE J. of Geotech. and Geoenviron. Engrg.*, 124(12): pp. 1211-1214
- Gray, D.H. and Ohashi, H. (1983). "Mechanics of Fiber-reinforcement in Sand", *ASCE J. Geotech. Engrg.* 109(3): pp. 335-353.
- Koutsourais, M., Sandri, D., and Swan, R. (1998). "Soil Interaction Characteristics of Geotextiles and Geogrids". *Proc. 6th Int. Conf. Geosynthetics*, Atlanta, Georgia, March 1998, pp. 739-744.
- Maher, M.H. and Gray, D.H. (1990). "Static Response of Sand Reinforced With Randomly Distributed Fibers", *ASCE J. Geotech. Engrg.* 116(11): pp. 1661-1677.
- Michalowski R.L., Cermak, J. (2003), "Triaxial compression of sand reinforced with fibers", *ASCE J. of Geotech. and Geoenviron. Engrg.*, 129(2): pp. 125-136
- Michalowski, R.L. and Zhao, A. (1996). "Failure of Fiber-Reinforced Granular Soils". *ASCE J. Geotech. Engrg.* 122(3): pp. 226-234.
- Ranjan, G., Vassan, R.M. and Charan, H.D. (1996). "Probabilistic Analysis of Randomly Distributed Fiber-Reinforced Soil", *ASCE J. Geotech. Engrg.* 120(6): pp. 419-426.
- Shewbridge, S.E. and Sitar, N. (1990). "Deformation Based Model for Reinforced Sand", *ASCE J. Geotechnical Engineering* 116(7): pp. 1153-1170.
- Zornberg, J.G. (2002) "Discrete framework for limit equilibrium analysis of fibre-reinforced soil", *Géotechnique* 52(8): pp. 593-604